

Alma Mater Studiorum Università di Bologna
Archivio istituzionale della ricerca

The role of mortar matrix in the bond behavior and salt crystallization resistance of FRCM applied to masonry

This is the final peer-reviewed author's accepted manuscript (postprint) of the following publication:

Published Version:

Franzoni E., Santandrea M., Gentilini C., Fregni A., Carloni C. (2019). The role of mortar matrix in the bond behavior and salt crystallization resistance of FRCM applied to masonry. CONSTRUCTION AND BUILDING MATERIALS, 209, 592-605 [10.1016/j.conbuildmat.2019.03.059].

Availability:

This version is available at: <https://hdl.handle.net/11585/707284> since: 2019-12-03

Published:

DOI: <http://doi.org/10.1016/j.conbuildmat.2019.03.059>

Terms of use:

Some rights reserved. The terms and conditions for the reuse of this version of the manuscript are specified in the publishing policy. For all terms of use and more information see the publisher's website.

This item was downloaded from IRIS Università di Bologna (<https://cris.unibo.it/>).
When citing, please refer to the published version.

(Article begins on next page)

This is the final peer-reviewed accepted manuscript of:

Elisa Franzoni, Mattia Santandrea, Cristina Gentilini, Alberto Fregni, Christian Carloni, *The role of mortar matrix in the bond behavior and salt crystallization resistance of FRCM applied to masonry*, Construction and Building Materials, Volume 209, 2019, Pages 592-605

ISSN 0950-0618

The final published version is available online at:

<https://doi.org/10.1016/j.conbuildmat.2019.03.059>

© 2019. This manuscript version is made available under the Creative Commons Attribution-NonCommercial-NoDerivs (CC BY-NC-ND) 4.0 International License (<http://creativecommons.org/licenses/by-nc-nd/4.0/>)

The role of mortar matrix in the bond behavior and salt crystallization resistance of FRCM applied to masonry

Franzoni Elisa^{a,*}, Santandrea Mattia^b, Gentilini Cristina^c, Fregni Alberto^a, Carloni Christian^d

^a DICAM – Department of Civil, Chemical, Environmental and Materials Engineering, University
of Bologna, Via Terracini 28, 40131 Bologna, Italy

^b DICAM – Department of Civil, Chemical, Environmental and Materials Engineering, University
of Bologna, Viale del Risorgimento 2, 40136 Bologna, Italy

^c DA – Department of Architecture, University of Bologna, Viale del Risorgimento 2, 40136
Bologna, Italy

^d Department of Civil Engineering, Case Western Reserve University, 10900 Euclid Ave,
Cleveland (OH), 44106, U.S.A.

Keywords: accelerated test; shear strength; salt crystallization cycles; water transport; porosity;
FRCM composite; interfacial debonding.

Abstract

Fiber-reinforced cementitious matrix (FRCM) composites are a new category of composites recently proposed for seismic strengthening of historical masonry structures, to provide a more compatible solution compared with fiber-reinforced polymer (FRP) composites. Despite the rapidly increasing number of research papers dealing with the mechanical behavior of FRCM composites applied to masonry, their long-term performance and susceptibility to weathering processes are still largely unexplored.

In this paper, the response of FRCM-masonry joints to accelerated weathering is investigated. A laboratory testing procedure, previously developed by the authors, which involves wetting-drying

* Corresponding author. Email: elisa.franzoni@unibo.it. Phone: +39 051 2090339

cycles in water and saline solutions, is employed.

Two different types of mortars (based on natural hydraulic lime and Portland cement) were used for the composite matrix, without changing the geometry, the type of masonry substrate and the fibers (galvanized steel cords), in order to assess the role of the matrix in the FRCM-masonry joint bond behavior and deterioration processes.

Results show that the matrix played a key role in the debonding mechanism of the FRCM-masonry joints as well as in the capillary absorption of water and in the resulting salt crystallization patterns.

1. Introduction

The improvement of the seismic response of historical masonry structures is of paramount importance to preserve the architectural heritage and protect people who live in historical constructions. The application of fiber-reinforced composites has been a breakthrough in the strengthening of masonry structures, such as vaults, domes, and walls, as these composites provide an increase of the collapse load without altering the mass of the structure and its aesthetical appearance. The latter aspect is very important for heritage buildings since several requirements, such as minimum intervention and reversibility, are imposed by the Restoration Charters [1].

Over the last decades, fiber-reinforced polymer (FRP) composites have been the most widely used composites for strengthening applications on historical buildings [2]. Their main advantages are the high-strength and high-stiffness to weight ratios and the relatively short curing time (few hours). Conversely, the sensitivity of FRPs to the condition of the masonry substrate (planarity, defects, residual moisture, etc.) [3, 4] and the ageing of the polymeric matrix [5] have been highlighted as possible critical issues in their short- and long-term performance, in addition to their limited resistance to high temperature and fire [6, 7] and partial detachment when subjected to aggressive salt crystallization cycles [7].

Fiber-reinforced cementitious matrix (FRCM) composites have been recently proposed to provide a more compatible and durable solution to strengthen masonry and concrete structures [8, 9]. The

term FRCM refers to composites that comprise different types of fibers (steel, glass, etc.) embedded within an inorganic matrix (cement, but also other hydraulic binders or even alkali activated materials [6, 10]). The major benefits of this new category of composites include their better resistance to high temperature, higher compatibility with masonry, and better durability with respect to FRPs [11]. Moreover, they can be employed even on irregular masonry substrates without the need of applying additional layers of mortar to smooth the surface and can be easily removed in case they need to be substituted (reversibility). The inorganic and porous nature of the matrix is considered a positive feature in terms of compatibility with masonry, because it allows water vapor diffusion, it has thermal and mechanical behavior similar to masonry and is not affected by the ageing processes typical of polymers. However, the durability of FRCM composites has not been fully investigated. The inorganic nature of the matrices exposes them to the risk of weathering mechanisms different from those affecting FRPs, such as those related to the presence of moisture in the pores of the inorganic matrix and substrate, e.g. freeze-thaw cycles and salt crystallization cycles [12-14]. Some previous studies investigated the effect of accelerated salt weathering on the performance of FRCM composites applied on brick and masonry [13] and on concrete [14]. These studies suggested that the deterioration and mechanical performance of FRCM composites is influenced by different parameters, including the nature of the matrix and the mechanical characteristics of the substrates [13], but the variability of results obtained by pull-off test did not allow to derive conclusive remarks [13-14]. The effect of salt crystallization on FRCMs was investigated in two previous papers by the authors [15,16], in which a procedure to reproduce in laboratory conditions capillary absorption and salt crystallization cycles in FRCM-masonry joints (i.e. masonry blocks strengthened with an FRCM composite strip) was developed. In those studies, masonry blocks were strengthened with strips of steel FRCM composites applied to one face and subjected to wetting-drying cycles in saline solutions and in deionized water for comparison. The saline solution was supplied from the face opposite to the one where the composite strip was

applied, in order to reproduce what usually occurs on-site, when masonry affected by rising damp and contaminated by salts is strengthened. Different lateral sealing configurations (total and partial wrapping with duct tape), saline solutions (aqueous solution of 8 wt% sodium sulfate decahydrate and a mixture of 8 wt% sodium sulfate decahydrate and 2 wt% sodium chloride), and number of cycles (4 and 6) were considered [15,16]. The adhesion between the composite and the masonry substrate before and after the cycles was investigated by performing single-lap shear tests. The FRCM composite employed, with natural hydraulic lime as binder, was found to be permeable to the flow of the saline solution, thus accumulation of salts beneath the composite did not occur and in turn its detachment was never associated with the presence of salts at the interface between the composite and the substrate. The steel cords exhibited signs of corrosion due to the presence of chlorides [16]. Composite strips were also applied to masonry blocks that previously underwent weathering cycles and therefore were salt contaminated, which appeared to be as harmful as salt crystallization cycles of the FRCM-masonry joints [16].

In this paper, the previously developed accelerated procedure to reproduce salt crystallization cycles [15, 16] was used to test different types of FRCM composites that were applied to the same masonry substrate. The first type employed the same natural hydraulic lime binder investigated in previous studies [15, 16], while the second type employed a Portland cement binder. The same steel fiber sheet was used for both composites. The second type of FRCM is suitable also for concrete strengthening [17-19]. As the fiber sheet was the same (galvanized steel cords) for both FRCM composites, the aim of this study was to investigate the role of the mortar matrix in the bond behavior of the FRCM-masonry joints in the presence of water and salts. The results show that the nature of the mortar changes completely not only the mechanisms of debonding, but also the water transport properties and salt accumulation patterns within the masonry blocks.

2. Materials and methods

2.1. Materials

The performance of the FRCM composite was determined in terms of adhesion capacity of the strips applied to a fired-clay brick masonry block, as this is widely recognized as the most realistic method to investigate the bond properties of the composite when applied to a masonry substrate [20].

The masonry blocks were constructed with 6 half solid fired-clay bricks ($55 \times 120 \times 125 \text{ mm}^3$) and 5 mortar joints (10 mm thick). The bricks were soaked in tap water for 1 hour before the masonry blocks were built, in order to prevent the absorption of the water from the joint mortar, which could lead to changes in the mortar properties [21]. The cut side of each brick was placed on the same face of the block. The mortar used for the joints was a commercially available dry-mix product made of natural hydraulic lime (compressive strength class NHL 3.5 according to EN 459-1 [22]) with quartz and dolomite aggregates ($< 2.5 \text{ mm}$).

Forty $120 \times 125 \times 380 \text{ mm}^3$ masonry blocks were constructed and left to cure for 1 month at room temperature and humidity. After 1 month, the FRCM composite strips were applied to one of the faces of the blocks. The face of the block with the cut side of each brick was not used to apply the FRCM strips. The fibers employed were arranged as a unidirectional sheet made of ultra-high strength galvanized steel cords, fixed to a secondary 6 mm-spaced fiberglass micromesh. The cross-sectional area and equivalent thickness of the cord are 0.538 mm^2 and 0.084 mm , respectively. The number of cords per unit width of the sheet is $0.157/\text{mm}$. The tensile strength, ultimate strain, and Young's modulus of the steel fibers are 3000 MPa, 2%, and 190 GPa, respectively. The fiber sheet was embedded in an inorganic mortar matrix and the total thickness of the composite was equal to 8 mm. The nominal dimensions of the FRCM-masonry joints are reported in Fig. 1a. The composite was applied according to the procedure described below:

- the masonry blocks were soaked in tap water for 1 hour;
- a first 4 mm-thick layer of mortar was applied to one face of the block, using a wood mold to define the bonded area;
- the steel fiber sheet was placed on the mortar layer and delicately pressed to ensure that the

cords were impregnated by the mortar;

- a second 4 mm thick layer of mortar was applied over the fiber sheet;
- the FRCM composite was left to cure for 28 days in laboratory, under a wet cloth in order to prevent excessive water evaporation and promote the mortar curing, then the artificial weathering protocol started.

Two different types of mortar were used as matrix of the FRCM system:

- a commercially available dry-mix mortar [23] made of natural hydraulic lime (NHL 3.5) and quartz sand that belongs to the strength class M15 according to EN 998-2 [24]. The composite and specimens that employ this mortar are labelled “NHL” in the remainder of the paper;
- a commercially available dry-mix mortar [25] made of Portland cement binder and quartz sand, with a limited amount of polymeric admixtures, and compressive strength > 45 MPa according to EN 12190 [26]. The FRCM that employs this matrix and the corresponding joints are labelled “CEM” in the remainder of the paper.

For both matrices, the amount of water recommended by the manufacturer was used to mix the mortar. These two matrices were selected for the present study because they were expected to have different behavior in terms of bond and salt weathering resistance of the composite.

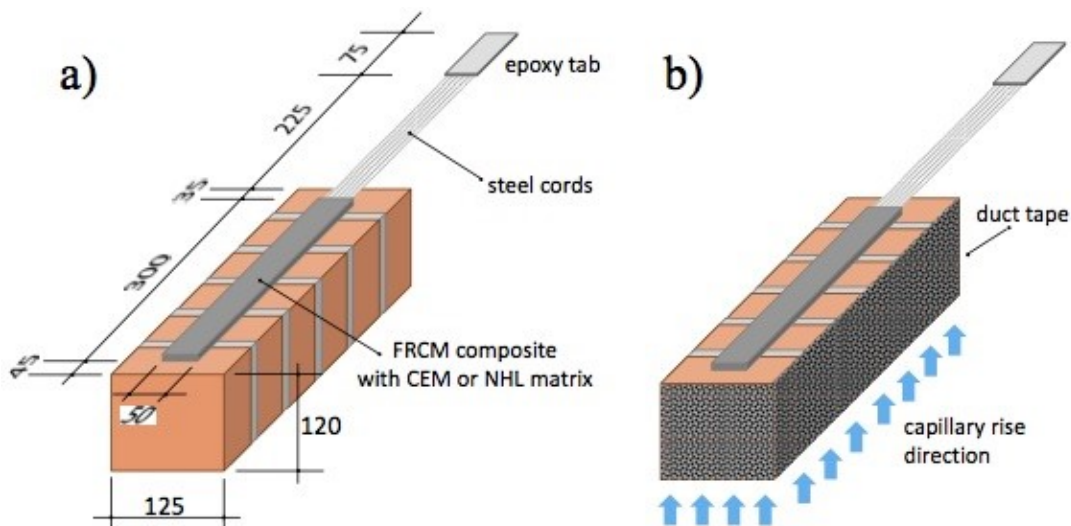


Figure 1. a) Sketch of the FRCM-masonry joints (dimensions in mm); b) Direction of the capillary rise of water or saline solution during the weathering cycles.

2.2. Accelerated artificial weathering

Setting-up an accelerated weathering test to assess the salt resistance of building materials is considered a very complex target. A recently-established RILEM Technical Committee (TC-ASC: Accelerated laboratory test for the assessment of the durability of materials with respect to salt crystallization) published a review paper about the critical parameters to be considered when salt crystallization cycles that occur in the field are attempted to be replicated in laboratory conditions [27]. Accelerating the salt damage without altering the deterioration mechanisms and patterns is very challenging, especially in the case of masonry, which is an assembly of different materials. To test the resistance to salt crystallization of masonry, the RILEM method MS-A.1 was proposed in 1998 [28]. Ten large wallettes are needed for each condition and 4 weeks are necessary for each cycle, so the procedure is time-consuming and requires a dedicated space in the laboratory. Moreover, the procedure was designed to test masonry alone and not masonry strengthened with composites, which requires specimens that are sufficiently small to handle, since they should be placed in a testing machine to conduct bond tests. Finally, the RILEM method MS-A.1 is very aggressive and its application to bricks and masonry blocks reinforced with FRCM composites in a previous study [13] produced a severe powdering of the pozzolanic lime-based mortar matrix and an extensive cracking of the cement-based one, hindering a proper determination of the residual adhesion bond of FRCM composite stripes. For all these reasons, an accelerated laboratory conditioning procedure specifically designed for FRCM-strengthened masonry blocks was recently proposed in [16]. This procedure involves cycles constituted by:

- a wetting phase, in which the specimens are partially immersed in a 20 mm head saline solution and allowed to absorb the liquid by capillarity as shown in Fig. 1b. To prevent evaporation, the lateral faces of the masonry blocks are wrapped with duct tape. The duration of the wetting phase is 2 days;

- a drying phase in a ventilated oven at 60 °C for 3 days.

The duration of the phases was set-up on the basis of preliminary tests [15]. In fact, it was found that deionized water took approximately 4 hours to reach the top surface of the specimens, hence 2 days were considered sufficient to produce a significant accumulation of salts on the top surface in lab environment (20 °C and RH 60%). The 3-day drying time in the oven was found to reduce the moisture content in the masonry blocks to less than 2%. Although such drying degree is not complete, it does not hinder the capillary absorption of the liquid in the subsequent wetting phase. A temperature of 60 °C in the oven was preferred with respect to the temperature indicated in EN 12370 [29] (105 °C), as it is considered more suitable for sodium sulfate crystallization tests [30]. The composition of the saline solution used in the present campaign was 2 wt% sodium chloride (NaCl) and 8 wt% sodium sulfate decahydrate ($\text{Na}_2\text{SO}_4 \cdot 10\text{H}_2\text{O}$). The amount of salts selected for the test was lower than the values suggested in EN 12370 [29] (14 wt% sodium sulfate decahydrate) and in RILEM test method MS-A.1 [28] (10 wt% sodium sulfate decahydrate and 10 wt% sodium chloride, separately). In fact, the purpose of the present test was to investigate the bond between FRCM composites and masonry affected by salt crystallization cycles, thus more ‘realistic’ conditions were preferred over highly aggressive cycles (as in EN 12370 [29], for example). For the same reason, a mixture of salts was used rather than a single type of salt and a total of 6 weathering cycles were carried out.

Four FRCM-masonry joints for each type of FRCM matrix were exposed to the accelerated salt damage procedure and were labelled “SALT”. Sixteen FRCM-masonry joints (8 for each matrix) were exposed to the same weathering cycles, but replacing the saline solution with deionized water. The need of investigating the influence of water and salts separately was pointed out in a previous study [31], where a possible beneficial effect of the water alone, used for the cycles, on the curing process of the mortar was highlighted. At the end of the 6th cycle in water, 8 FRCM-masonry joints (4 for each matrix) were dried in oven at 60 °C and let to cool down at laboratory conditions. These specimens were labelled “WAT”. The other 8 specimens (4 for each matrix) were immersed in

deionized water for 2 additional days and then tested in saturated conditions. These specimens were labelled “WAT-SAT”. This last group of specimens was used to investigate the role of the water saturation of the pores on the composite/substrate adhesion, independently of salts, which has been highlighted as an important issue for materials performance [31-37].

A group of 8 FRCM-masonry joints (4 for each matrix) was not subjected to any cycle and after the 28 day curing period was left in the laboratory for the entire duration of the accelerated weathering test. These specimens were labelled “REF” and were used as control specimens.

Finally, an additional condition was investigated. As FRCM composites might be applied to masonry structures that are already contaminated with salts, 8 masonry blocks (4 for each matrix type) were exposed to weathering cycles in the saline solution before the composite strip was applied. At the end of the 6th cycle, the top surface of the specimens was cleaned by means of a steel brush to remove the efflorescence and any crumbling part. Then, the composite was applied, following the same procedure described above. The FRCM-masonry joints were tested right after the composite was cured for 28 days (under a wet cloth) and allowed to dry out. These specimens were labelled “SALT-BEFORE”.

All the weathering conditions of the FRCM-masonry joints are summarized in Table 1.

Prior to carrying out any test, all FRCM-masonry joints, except the WAT-SAT specimens, were oven dried at 60 °C for 2 days, to eliminate any possible residual moisture from the previous conditioning procedures, and then allowed to cool down at laboratory conditions.

Table 1. Labels of the tested FRCM-masonry joints.

Type of matrix of the composite strip		Conditioning	Number of specimens
Cement-based mortar	NHL-based mortar		
CEM-REF	NHL-REF	No cycles (kept at laboratory conditions)	4 (CEM) + 4 (NHL)
CEM-WAT	NHL-WAT	Six cycles in deionised water and at the end of the cycles drying	4 (CEM) + 4 (NHL)
CEM-WAT-SAT	NHL-WAT-SAT	Six cycles in deionised water and at the end of the cycles water saturation	4 (CEM) + 4 (NHL)
CEM-SALT	NHL-SALT	Six cycles in saline solution and at the end of the cycles drying	4 (CEM) + 4 (NHL)
CEM-SALT-BEFORE	NHL-SALT-BEFORE	Six cycles in saline solution before the composite application	4 (CEM) + 4 (NHL)

2.3. Characterization techniques

The compressive and flexural strengths of the two matrix mortars were determined using 6 $40 \times 40 \times 160 \text{ mm}^3$ mortar prisms (3 for each matrix) that were cast from the same batch of mortar used to apply the FRCM strips. The mortar prisms were left to cure under a wet cloth for 28 days (as the composite strips in the FRCM-masonry joints) and then left in laboratory conditions for the entire duration of the weathering cycles. Flexural and compression tests according to EN 1015–11 [38] were conducted at the time when direct shear tests of the FRCM-masonry joints were performed, so that their age (prisms and specimens) was comparable.

The determination of the capillary water absorption coefficient, CA (also known as sorptivity), of the bricks and matrix mortars used in this study, was carried out according to EN 15801 [39] on the half-bricks and the above mentioned mortar prisms, respectively. The bulk density was determined for the same samples, as the ratio between the dry weight and the volume.

At the end of the artificial weathering cycles in water and in saline solution, a visual assessment of the efflorescence distribution and of possible deterioration of the surface of the specimens was carried out. Afterwards, direct shear tests were performed to assess the bond quality between the FRCM composite and the masonry blocks. Details of the set-up of the single-lap shear tests are reported in [15, 40]. During the tests, the masonry specimens were restrained between two 20 mm-thick steel plates, while the composite strip was pulled. The bottom plate was connected to the lower grip of the testing machine and the upper one was connected to the bottom plate by means of four threaded rods. The load P was applied to the end of the bare fibers outside the bonded area of the composite. Two linear variable displacement transformers (LVDTs) were mounted on the face where the composite was applied to measure the displacement of the composite with respect to the masonry surface at the beginning of the bonded area. The average of the two LVDT readings is named global slip g in this work. All tests were conducted in displacement control at a constant global slip rate equal to $0.84 \text{ }\mu\text{m/s}$ until failure.

After the shear tests were performed, small fragments of bricks and composite matrices were removed by a chisel in some key locations of the specimens, namely:

- from the internal layer of matrix (between the steel cords and the masonry surface);
- from the external layer of matrix (between the steel cords and the external surface of the composite), after the efflorescence (if any) were removed by dry brushing the composite surface;
- from a brick beneath the composite strip;
- from a brick surrounding the bonded area, near the top surface. The sample was carefully extracted removing first a thin layer of the brick surface, where the presence of efflorescence might have affected the results.

Further details about the sampling locations are given in Section 3.4, where the results are discussed.

These fragments of brick and matrices were used to determine the salt amount by ion chromatography (IC), in order to investigate the distribution of the salts inside the FRCM-masonry joints. IC was performed in a Dionex ICS-1000, after grinding the sample to powder (<0.075 mm), extracting the soluble salts with deionized boiling water (electrical conductivity <0.02 μ S), and filtrating by blue ribbon filter. Two samples per specimen type, extracted from different FRCM-masonry joints, were analyzed for each location and the results were averaged.

Mercury intrusion porosimetry (MIP) was carried out first on fragments of the unweathered materials (NHL matrix, CEM matrix and brick), which were sampled from the corresponding REF specimens, to investigate how their porosities differ. Then, MIP was performed on the fragments of the NHL matrix and CEM matrix collected from the upper layer of the composite strips, after the weathering cycles, with the aim of investigating the possible deterioration of the matrices due to cracks opening. MIP was performed in a Porosimeter 2000 with a Fisons Macropore Unit 120, directly on the fragments collected.

Moreover, after the shear tests were performed, a strip of the internal layer of the composite was

separated from the masonry substrate by hitting the mortar with a chisel along the masonry-matrix interface. After removing the steel fibers and fiberglass mesh residues, mortar samples were cut to obtain regular $50 \times 50 \times 4 \text{ mm}^3$ thin plates, which were used to determine the capillary water absorption coefficient. Given the small thickness of the samples, it was impossible to place them vertically on a wet filter paper pack as requested in EN 15801 procedure [39]. Thus, each sample was hung in a vertical position and a large tray with deionized water was placed under it, so that the water surface touched the bottom of the sample. The mass increase of the sample was recorded as a function of time.

Finally, after the direct shear tests were performed, the steel fibers in the composites were also visually observed to evaluate the possible presence of surface alterations of the cords.

3. Results and discussion

3.1. Mechanical properties of the matrices

The average compressive strength of CEM matrix and NHL matrix resulted equal to 46.9 MPa (CoV=8.5%) and 13.5 MPa (CoV=6.5%), respectively. CEM matrix exhibited a compressive strength more than three times higher compared with the natural lime-based matrix. The average flexural strength resulted equal to 7.2 MPa (CoV=19.2%) for CEM mortar and 4.7 MPa (CoV=0.1%) for NHL mortar.

3.2. Efflorescence distribution on the FRCM-masonry joints after the weathering cycles

After 6 wetting-drying cycles in deionized water, for both groups of specimens CEM-WAT and NHL-WAT, a slight efflorescence formation was observed on the top masonry surface, near the edges, where water evaporation rate was higher (Fig. 2a and b, respectively). In fact, although the duct tape hindered the evaporation through the side surfaces, its sealing action along the edges was not perfect, as the oven drying cycles made the tape detach slightly from the edges. These slight efflorescence were due to some salt impurities originally present in the materials (see Section 3.4).

In the NHL-WAT specimens (Fig. 2b), the composite strip was covered by a slight and irregular layer of efflorescence, while the composite surface in the CEM-WAT specimens (Fig. 2a) was totally free of any efflorescence.

After 6 cycles in saline solution, for the CEM-SALT specimens, the top surface of masonry on each side of the composite was almost entirely covered by salts, while the composite was efflorescence free (Fig. 2c). Conversely, the accumulation of salt crystals on the top surface was evident for NHL-SALT specimens (Fig. 2d), where efflorescence was present on the composite and masonry (especially near the composite) surfaces. These very different salt accumulation patterns suggest that the migration paths of the saline solution through the FRCM-masonry joints depend on the type of composite (as it will be explained in Section 3.4).

The SALT-BEFORE masonry blocks were covered by a uniform layer of efflorescence after the end of the cycles (Fig. 3a and b), which confirms that the experimental set-up provides a unidirectional capillary flow of the saline solution toward the top surface. After the FRCM composite was applied and cured under wet clothes, the matrix dried out and the salts previously accumulated inside the blocks migrated toward the surface and caused a thick layer of efflorescence on the composite surface of the NHL-SALT-BEFORE specimens, which was covered by salt crystals (Fig. 3d and f). Conversely, the composite surface of the CEM-SALT-BEFORE specimens was efflorescence free (Fig. 3c and e).



Figure 2. Photos of representative: a) CEM-WAT, b) NHL-WAT, c) CEM-SALT and d) NHL-SALT specimens at the end of the 6th cycle.

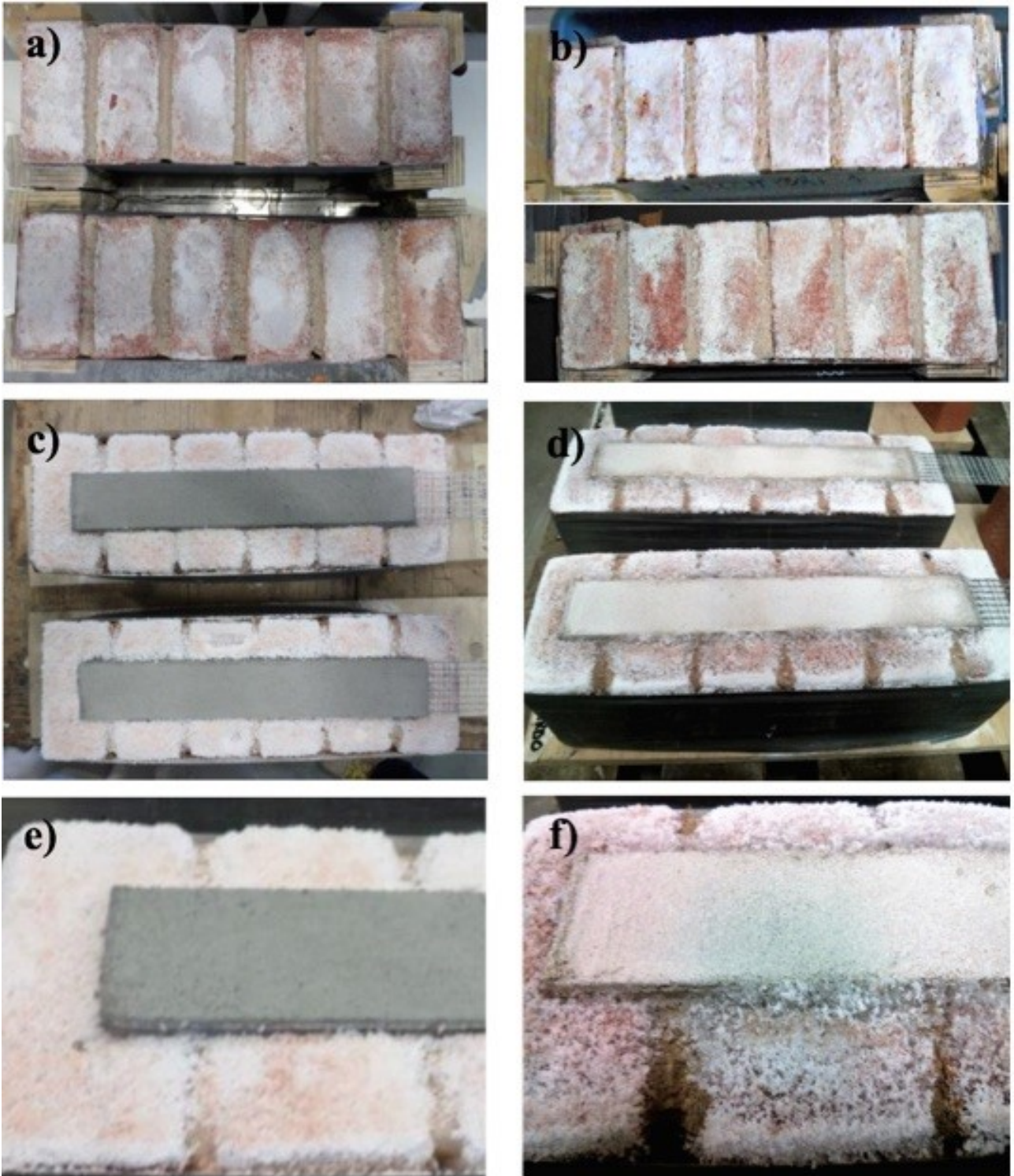


Figure 3. Photos of representative a) CEM-SALT-BEFORE, b) NHL-SALT-BEFORE masonry blocks at the end of the 6th cycle before the composite application; (c, e) CEM-SALT-BEFORE, (d, f) NHL-SALT-BEFORE specimens at end of the composite curing.

3.3. Single-lap shear test

The results of single-lap shear tests for CEM-REF and NHL-REF specimens in terms of applied load P versus global slip g curves are shown in Fig. 4a and b, respectively. For the sake of clarity,

in Fig. 4c and d and in the following ones, results obtained from the experimental tests performed on the reference and conditioned specimens are reported as envelope curves. For both CEM-REF and NHL-REF specimens, the load versus global slip response is characterized by an initial linear portion followed by a non-linear branch until either an absolute peak load is reached or a relative peak load is attained followed by a series of load drops. For the majority of the reference specimens, after the peak load is reached, a drop in the load response marks the onset of a nominally constant branch (plateau). For most of the CEM specimens, the constant load branch is characterized by sudden drops followed by ascending portions and subsequent drops until failure (see Fig. 4a). The failure mode that characterized CEM-REF specimens was debonding at the matrix-substrate interface, with a thin layer of masonry that remained attached to the composite strip (Fig. 5a). This failure mode is typical of FRP-masonry joints; while the failure mode of NHL-REF specimens was interlaminar failure at the matrix-fibers interface, as shown in Fig. 5b. For NHL-REF specimens, the crack propagates in a self-similar manner at the fiber-matrix interface, which results in a plateau in the corresponding P - g curve. For CEM-REF specimens, since the crack involves the masonry substrate, the plateau trend is interrupted by load drops due to the non-homogeneous (periodically variable) nature of the substrate composed by bricks and mortar joints [41]. The average absolute maximum load (indicated as P_{avg}^*) for each group of specimens is reported in Fig. 6. It should be noted that data for NHL specimens are taken from [16]. As expected for this class of materials, for both CEM-REF and NHL-REF specimens, results show some variability that may be due to several factors such as the specimen/composite casting and curing conditions. Notwithstanding this variability, a general trend can be noted for both CEM and NHL specimens. Comparing the CEM-REF specimens (Fig. 4a) and the NHL-REF specimens (Fig. 4b), it can be observed that, on average, they reached similar values of the peak load (Fig. 6).

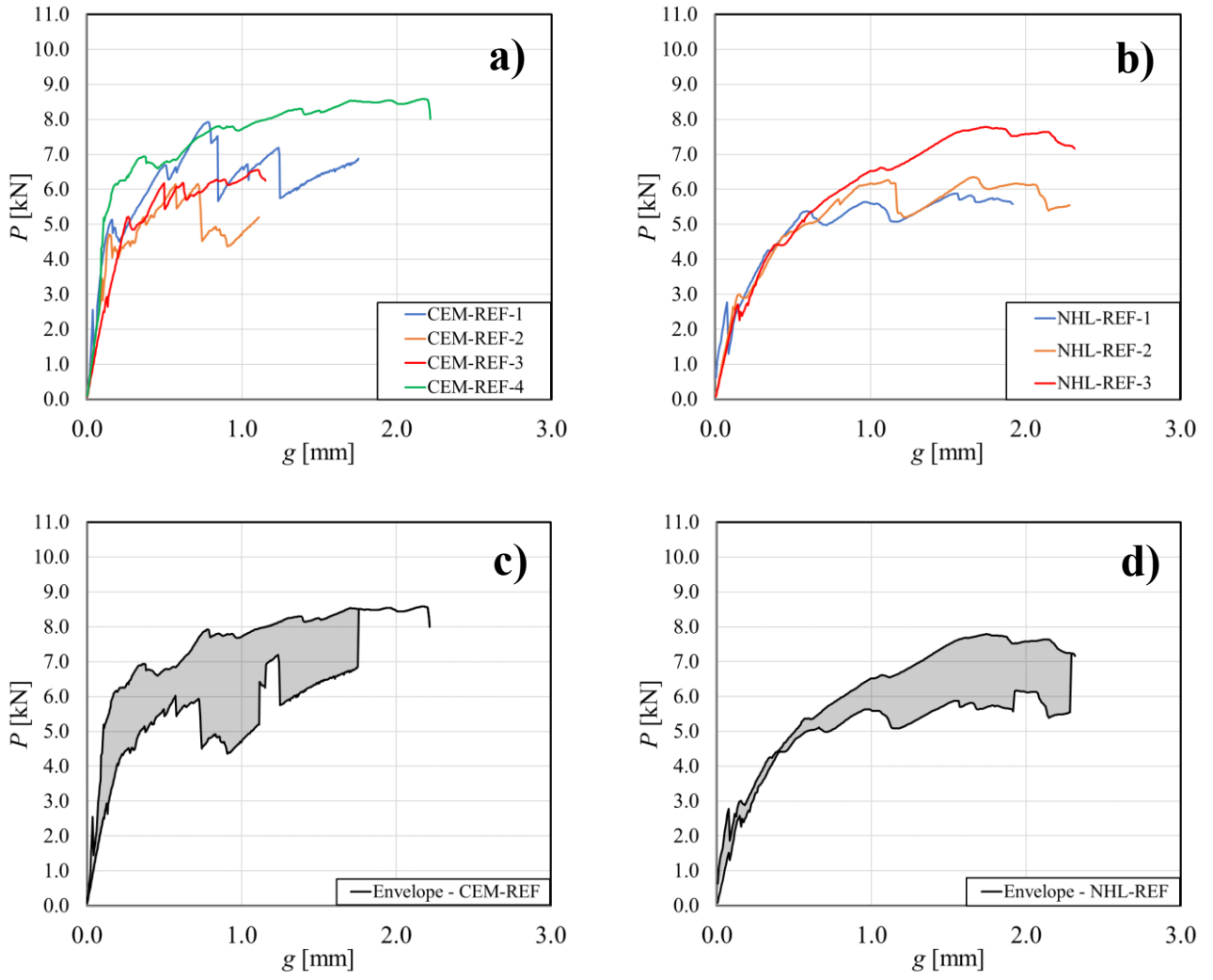


Figure 4. Applied load P - global slip g curves of a) CEM-REF and b) NHL-REF specimens (the P - g curve for NHL-REF-4 specimen is not reported due to an anomalous behavior of the specimen during the test procedure); Envelope curves for c) CEM-REF and d) NHL-REF specimens.

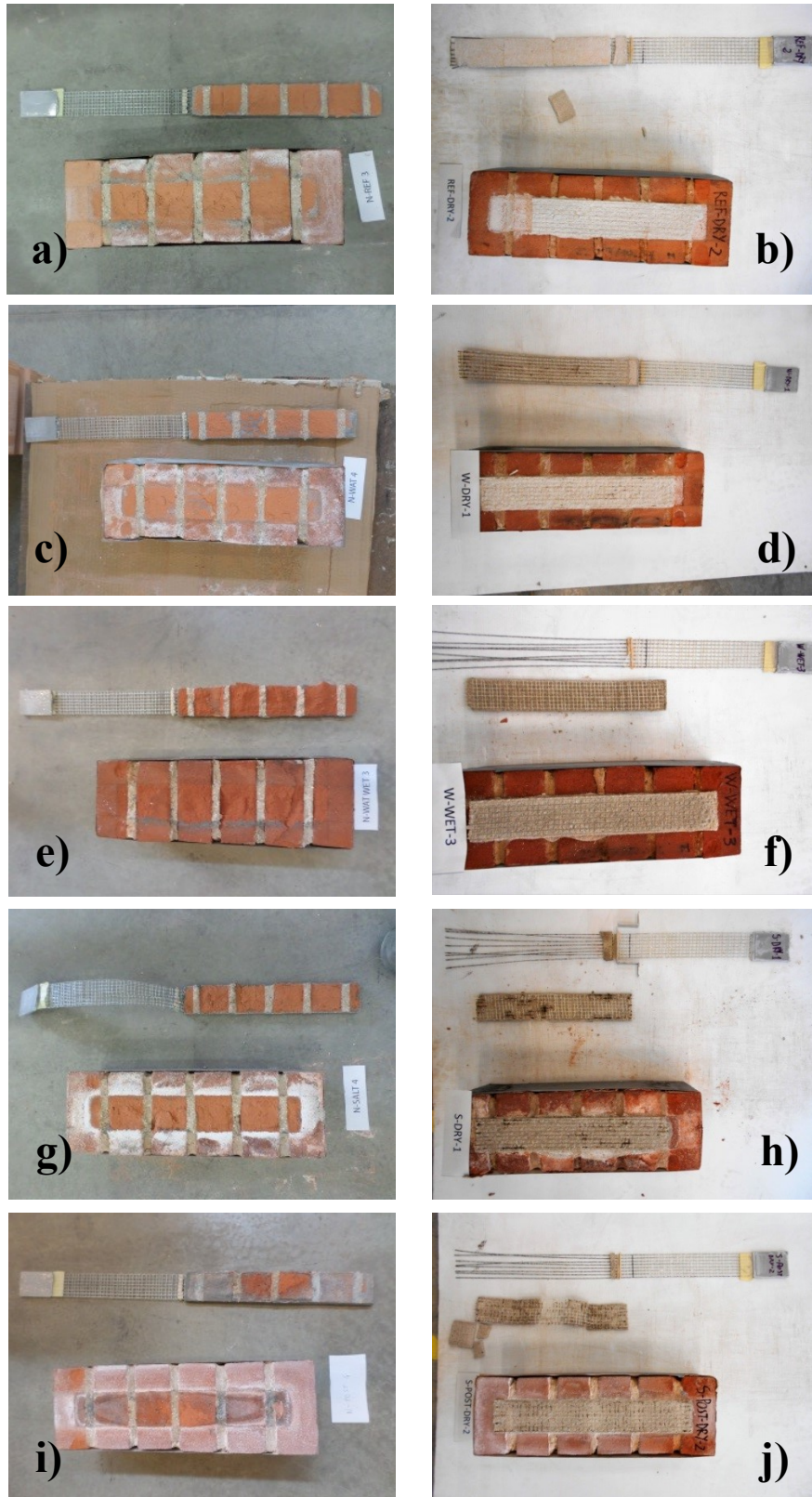


Figure 5. Failure modes of representative a) CEM-REF, b) NHL-REF, c) CEM-WAT, d) NHL-WAT, e) CEM-WAT-SAT, f) NHL-WAT-SAT, g) CEM-SALT, h) NHL-SALT, i) CEM-SALT-BEFORE and j) NHL-SALT-BEFORE specimens.

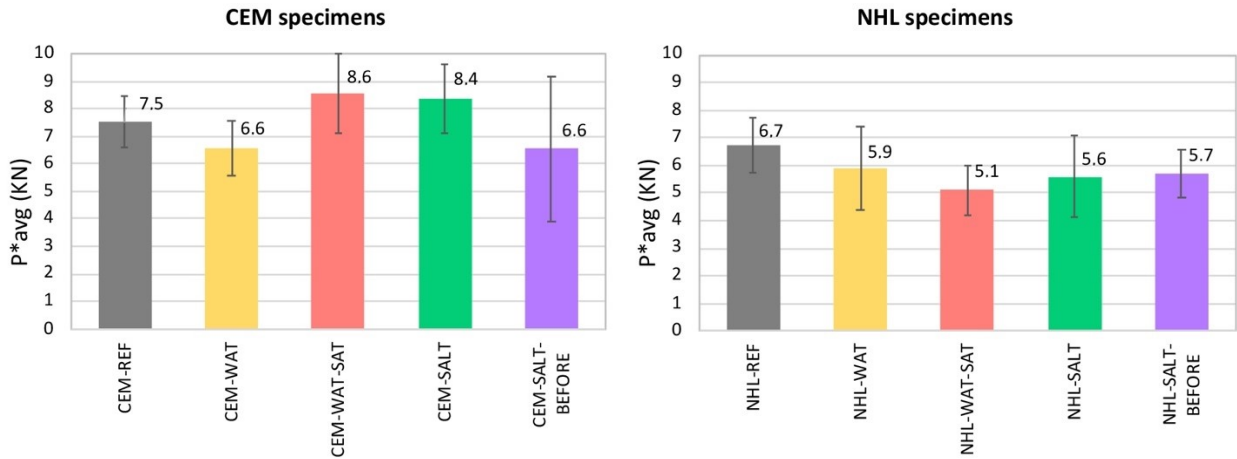


Figure 6. Results of the direct shear tests in term of average peak load, P^*_{avg} , for each group: a) CEM specimens: b) NHL specimens. Data for NHL specimens are taken from [13].

Both CEM-WAT and NHL-WAT specimens (Fig. 7a and b, respectively, and Fig. 6) show similar load responses with respect to the corresponding REF specimens, with a smaller value of peak load for both CEM and NHL specimens that cycled in water (-12%). These results suggest that the curing procedure employed for these composites was such to allow a full development of the mechanical and physical characteristics of the mortar, i.e. the water in the cycles did not contribute substantially to the curing process. Also the failure modes remained the same with respect to REF specimens (Fig. 5c for CEM-WAT and Fig. 5d for NHL-WAT).

No remarkable difference was observed in the P - g curves between CEM-WAT-SAT and CEM-REF specimens (Fig. 7c), as the fracture surface involved the bricks, where the pore saturation was demonstrated not to have a significant effect on strength, although only compressive strength was investigated [32]. Conversely, NHL-WAT-SAT specimens show a non-negligible decrease (-24%) in the value of P^*_{avg} with respect to NHL-REF specimens (Fig. 6 and Fig. 7d). This fact is probably due to the presence of water in the pores of the matrix mortar, which facilitated the fracture formation and propagation [35-37].

The load responses of CEM-SALT specimens are similar to the load responses of CEM-REF specimens (Fig. 6 and Fig. 8a), which indicates that the salt crystallization in the masonry substrate after the application of the composite strip did not affect the bond behavior; this aspect will be

further investigated in Section 3.4, where the solution flow patterns and salt concentration within the specimens are presented. NHL-SALT specimens show a lower bond quality than NHL-REF specimens (Fig. 8b and Fig. 6), since the weathering cycles with the saline solution caused some corrosion on the steel cords, due to the presence of sodium chloride, as observed in [16]. Due to the steel corrosion, the fiber-matrix interface resulted weaker and a lower amount of energy was needed to initiate and propagate the interfacial crack. For CEM-SALT specimens no corrosion was observed in the steel fibers (Fig. 9).

The CEM-SALT-BEFORE envelope appears lower with respect to the reference envelope, even if in terms of peak values the decrease is not particularly significant, -12% (Fig. 6 and Fig. 8c). At failure, the composite strip of CEM-SALT-BEFORE specimens detached from the masonry substrate with a very thin layer of masonry attached (Fig. 5i). The layer of masonry attached was much thinner than the layer observed for CEM-REF specimens (Fig. 5a). In the case of CEM specimens, the adhesion of the composite to the masonry substrate is highly affected by the substrate preparation. The presence of salts in the pores of masonry prior to applying the composite strip could entail for a reduced peak load value. The bond behavior of NHL-SALT-BEFORE specimens is similar to NHL-SALT specimens, i.e. lower than NHL-REF specimens (Fig. 6 and Fig. 8d). This result shows that, for NHL specimens, the application of the composite strip to a salt-laden substrate or the exposure of a FRCM-masonry joint to salt crystallization cycles lead to similar bond behaviors.

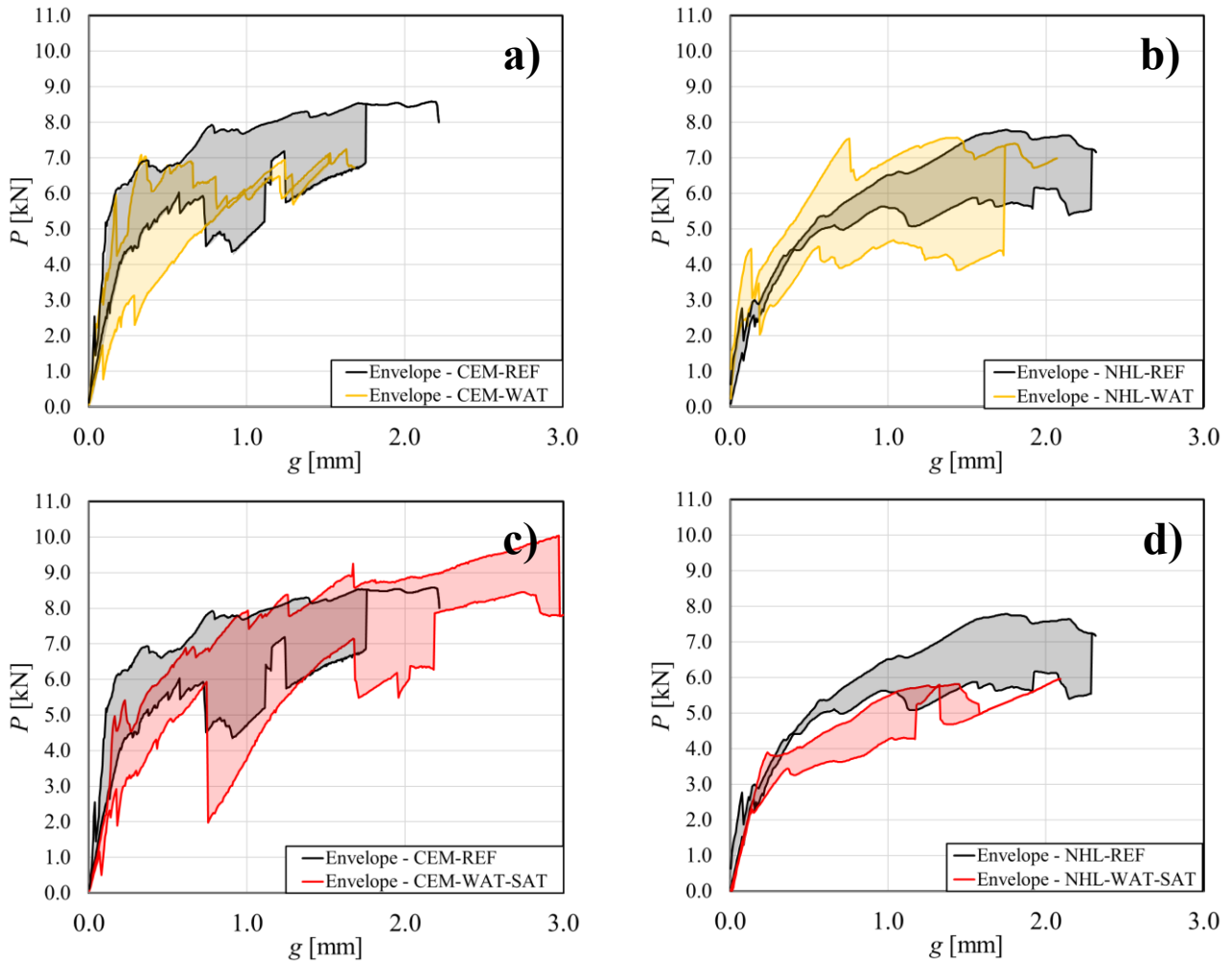


Figure 7. Applied load P - global slip g envelope curves of a) CEM-WAT, b) NHL-WAT, c) CEM-WAT-SAT, d) NHL-WAT-SAT specimens (REF envelope curves are reported for comparison).

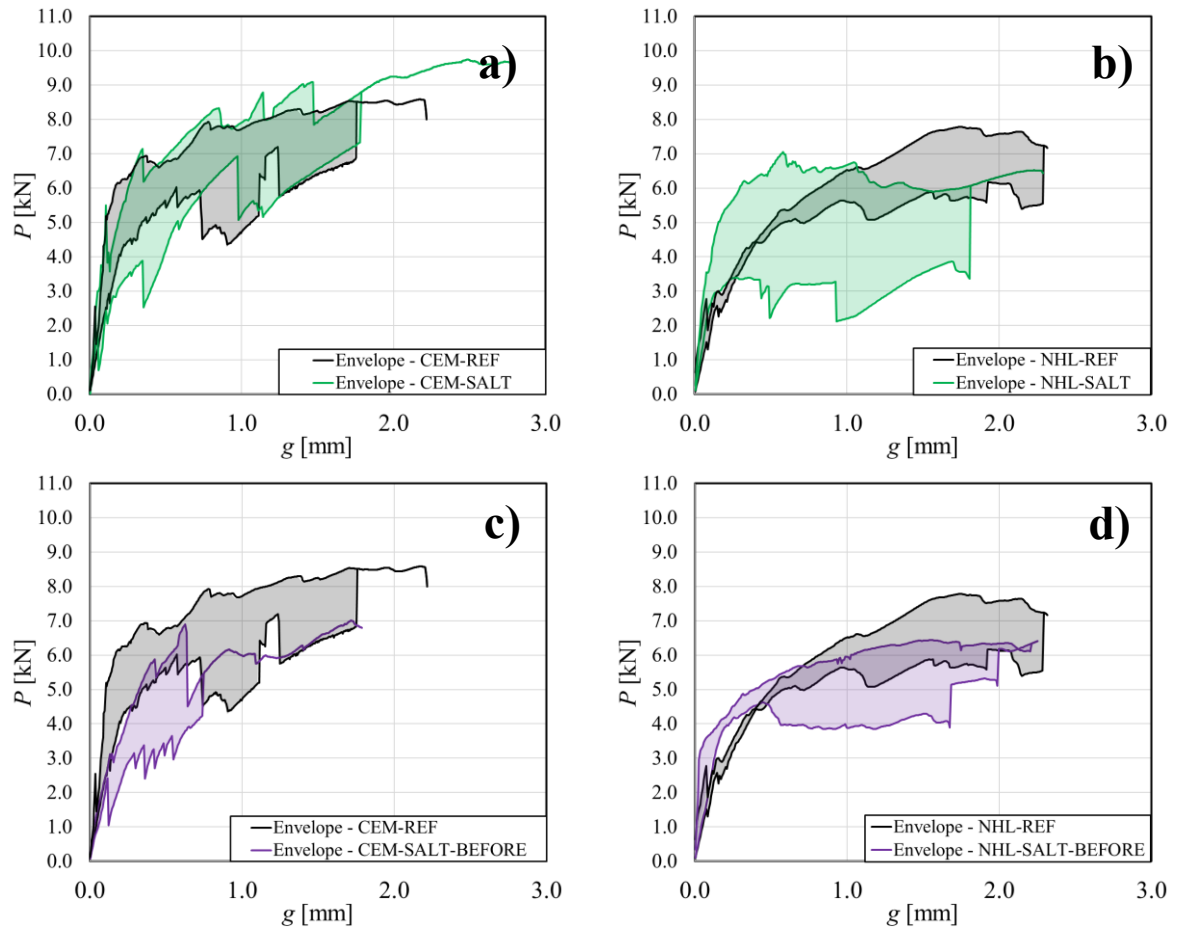


Figure 8. Applied load P - global slip g envelope curves of a) CEM-SALT, b) NHL-SALT, c) CEM-SALT-BEFORE and d) NHL-SALT-BEFORE specimens (envelope curves are reported for comparison).



Figure 9. Details of the steel fibers in the composite after the shear test in a CEM-SALT specimens where no surface alterations and/or corrosion are visible.

In summary, when NHL matrix is employed, failure always occurs within the composite, namely at the fiber-matrix interface, which also results in a smooth and regular response. When the cementitious matrix is employed, failure shifts from the matrix-fiber interface to the composite-masonry interface. In FRCM composites bonded to quasi-brittle materials, the fracture surface could occur within the composite as the two layers of matrix separate, at the matrix-substrate interface with a neat separation between materials or within the substrate in a cohesive manner. The hierarchy of fracture surfaces depends on the energy required to activate each surface. The weaker surface, i.e. the surface with the least amount of energy required, will be the one where fracture occurs, as pointed out in [41]. The role of the substrate (quality, planarity, salt presence) becomes more important, as in the case of FRP composites, when failure occurs at the composite-substrate interface. The different location of the fracture surface is also the reason why, despite the use of matrices of so different compressive strengths, the peak loads of the reference FRCM-masonry joints are very similar between the two groups of specimens (Fig. 6).

3.4. Microstructure, moisture transport properties and salt distribution in the masonry joints

The capillary absorption curves of the unweathered materials, i.e. brick, NHL and CEM mortar prisms, are reported in Fig. 10. It should be noted that the maximum absorption value achieved by the brick should not be compared with the values of the mortars, due to the different height of the samples. The values of capillary water absorption coefficient (CA or sorptivity) of the same samples are reported in Table 2. Table 2 also reports the CA values of NHL and CEM mortar fragments (plates) collected from NHL-REF and CEM-REF specimens, respectively. In fact, the microstructure of the mortar might be affected by the application method (casting in steel molds in the case of prisms, or application onto the masonry surface in the case of the composite strip), so CA was determined for both kinds of samples. The pore size distribution curves obtained by MIP analysis on fragments collected from the FRCM-masonry joints (REF samples) are represented in

Fig. 11 and the values of total open porosity (OP) and pore mean radius (R_{mean}) found by MIP are reported in Table 2.

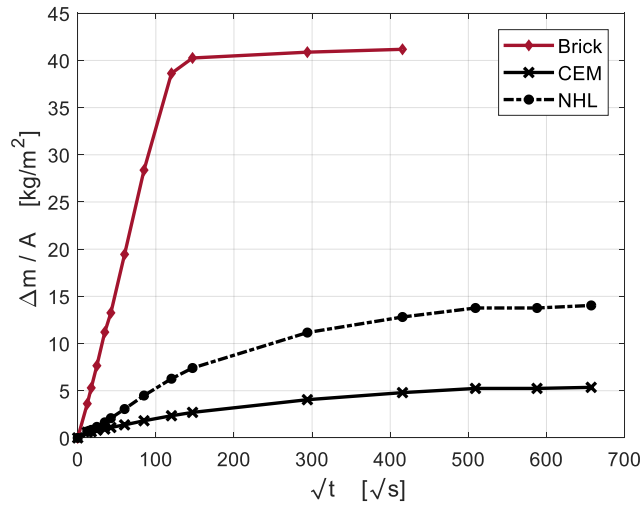


Figure 10. Capillary water absorption curves of the brick and matrices (determined on half-brick and mortar prisms cast in molds).

Table 2. Results of the microstructural characterisation and water transport properties of the two composite matrices (CEM and NHL) and brick. ^a = determined on the mortar prisms casted in steel molds; ^b = determined on the matrix layers taken from CEM-REF and NHL-REF specimens; ^c = determined by MIP.

Sample	Bulk density ^a (kg/m ³)	CA (kg/m ² s ^{1/2})		OP ^c (%)	R_{mean} ^c (μm)
NHL mortar	1898 ^a	0.054 ^a	0.050 ^b	26.6 ^b	0.491 ^b
CEM mortar	2005 ^a	0.020 ^a	0.031 ^b	22.5 ^b	0.041 ^b
Brick	1679	0.327		43.0	0.848

The results highlight a strong difference between brick, NHL matrix, and CEM matrix in terms of porosity and water transport properties. The brick exhibits the highest porosity (43%), mean pore radius equal to 0.848 μm (Table 2) and a unimodal pore size distribution curve, which is typical for this type of material that exhibits the majority of pores with ≈ 1 μm radius (Fig. 11). Consistently, the capillary absorption curve of brick (Fig. 10) is first linear and then quickly reaches a plateau, which corresponds to the saturation of the pores, which is again typical for fired-clay bricks. NHL and CEM matrices exhibit a much lower porosity (26.6% and 22.5%, respectively, Table 2) and a completely different pore size distribution with respect to fired-clay bricks. NHL has a smaller R_{mean} (0.491 μm) with respect to brick, and pores within the full range 0.0035-0.5 μm (Fig. 11). CEM

matrix exhibits much finer pores ($R_{mean} = 0.041 \mu\text{m}$, i.e. an order of magnitude smaller than NHL), with a prevalence of pores $< 0.1 \mu\text{m}$ (Fig. 11). Consistently, the two matrices display a slow initial water absorption (linear part of the curves in Fig. 10) and then a gradual saturation, due to the progressive filling of the fine pores. Given its lower porosity and smaller R_{mean} with respect to NHL, CEM obviously exhibits a smaller sorptivity value (less than half). It is important to note that the sorptivity of the two matrices resulted basically the same when determined on mortar prisms and fragments extracted from the composite, which confirms that wetting the masonry blocks before the application of the composite and during its curing process (under a wet cloth) were effective expedients to prevent the premature depletion of the water from the matrices.

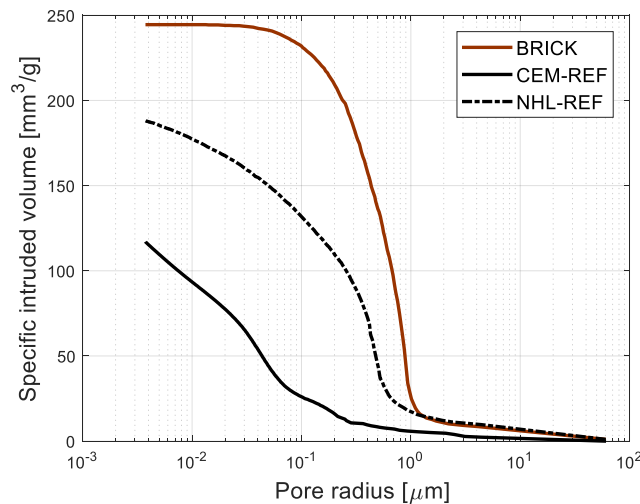


Figure 11. MIP curves of the brick and matrices (samples collected from CEM-REF and NHL-REF specimens).

MIP analysis was carried out also on the fragments of the matrix extracted from the composite of WAT, SALT, and SALT-BEFORE specimens (upper layer of matrix in the composite strip), for both kinds of matrix. The results are reported in Fig. 12. Remarkable differences can be observed between the two mortars. A limited variation of porosity occurred in CEM matrix after the conditioning (Fig. 12a). Cycles in water produced no effect (CEM-WAT) and also the pore clogging effect due to salts (CEM-SALT and CEM-SALT-BEFORE) is just barely noticeable. This suggests that the absorption of the saline solution by CEM matrix was limited, as well as the

relevant salt accumulation. This aspect was further investigated by determining the salt distribution in the specimens by IC. On the contrary, the matrix of NHL-WAT is only slightly less porous than the REF one, but its porosity can be considered basically comparable, as the difference observed is basically due to pores with radius $> 3 \mu\text{m}$ and hence might be affected by some occasional large void embedded in the mortar during its mixing and application. After the cycles in the saline solution (NHL-SALT, Fig. 12b), the NHL matrix exhibits a clear decrease in porosity, owing to salt accumulation in the pores. No evidence of new crack opening due to salt crystallization cycles was found. Even more evident is the pore-filling effect in the matrix of NHL-SALT-BEFORE specimens, in which the porous matrix seems to have behaved like a ‘poultice’ [42] that absorbed the salts from the underlying salt-laden masonry block, despite the preventive removal of the efflorescence from the surface with a brush.

IC results are graphically presented in Figs. 13 and 14 for the sake of clarity. Average values and standard deviations are reported for each sampling location. The original materials (collected by REF specimens) contain small amounts of salts, which is quite common for bricks and mortars. Both matrices exhibit a higher saline content than the brick with a predominant presence of sulfate (about 0.5 wt% in NHL-REF, Fig. 13, and 0.9 wt% in CEM-REF, Fig. 14), due to impurities in the raw materials and/or to the gypsum fraction in the cement.

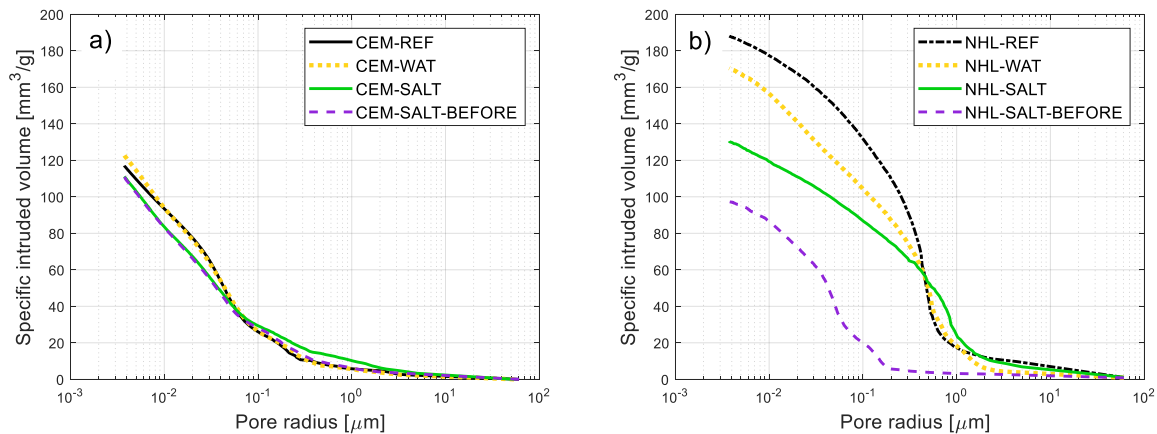


Figure 12. MIP curves of a) CEM and b) NHL matrices, collected from the composite in the FRCM-masonry joints.

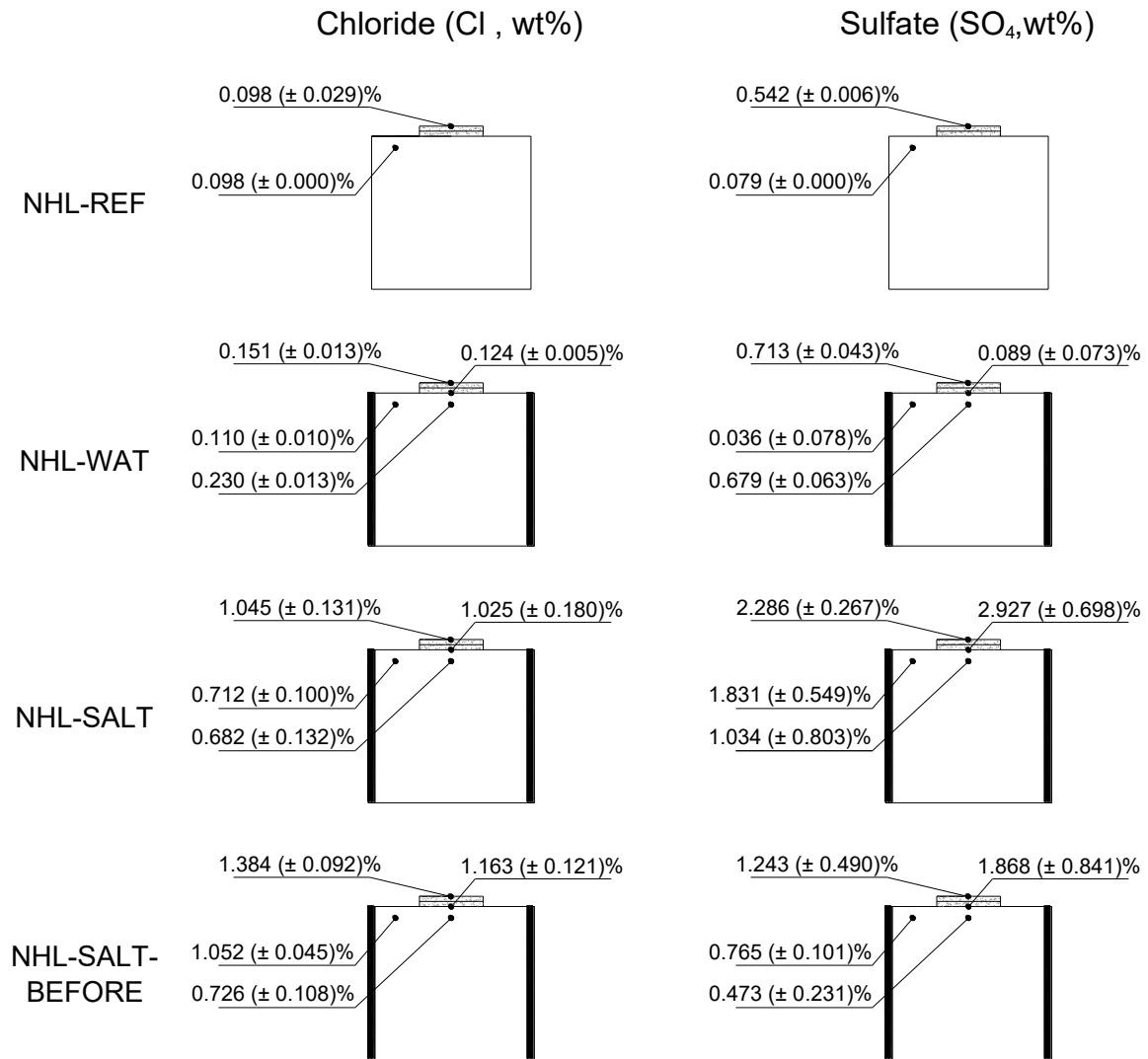


Figure 13. Anions amounts in selected locations of the NHL specimens.

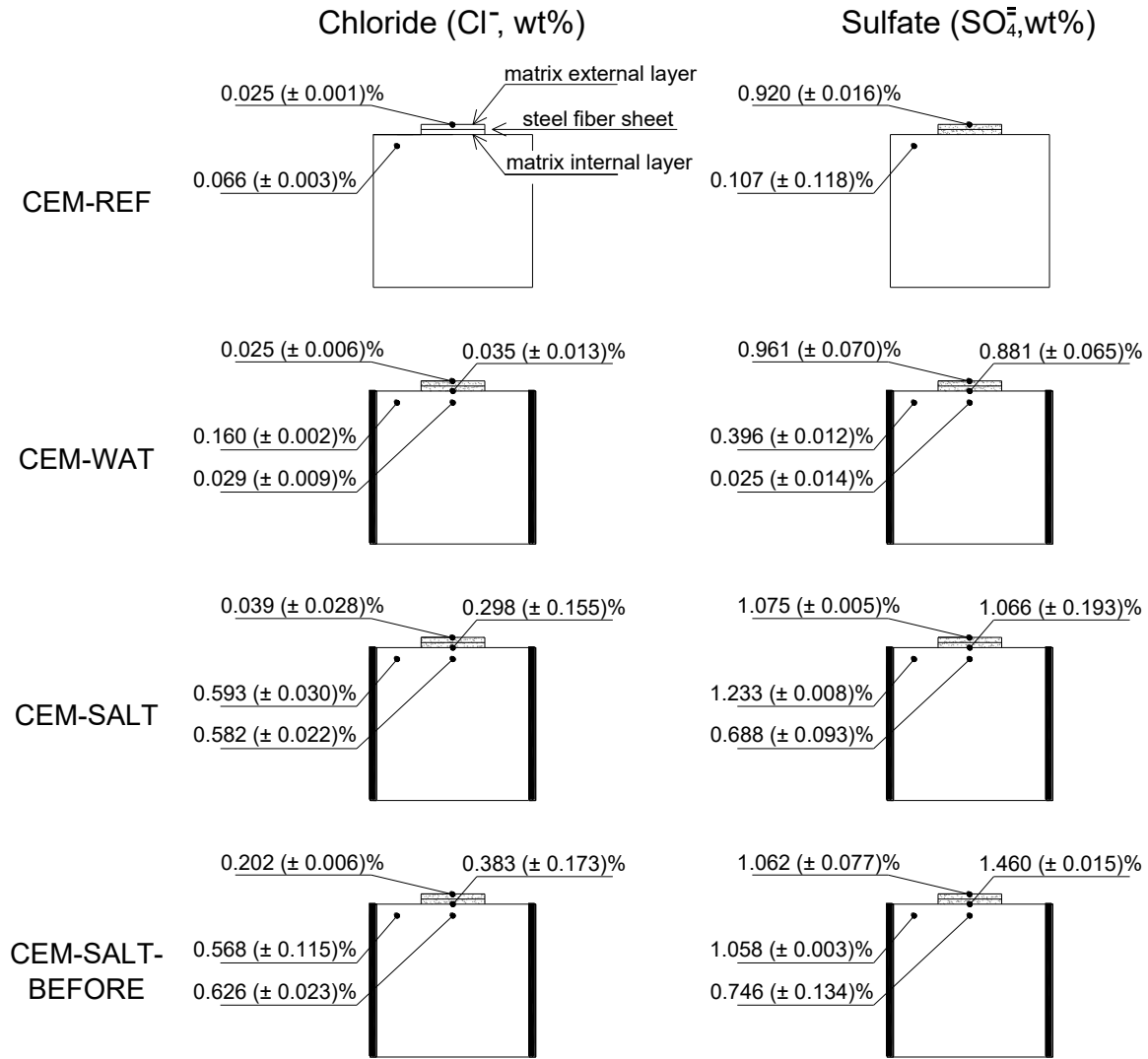


Figure 14. Anions amounts in selected locations of the CEM specimens.

In NHL specimens (Fig. 13), the cycles in deionized water caused the dissolution of the salts originally present in the materials and their migration toward the top surface, hence a slight enrichment of anions was found in NHL-WAT composite (more evident for sulfate anions, due to their higher amount). This suggests that the composite strip, due to its high porosity, does not alter significantly the capillary water flow, which is basically unidirectional. The same behavior is observed in NHL-SALT specimens, where the highest salt amount was found in the composite rather than in the brick, with no particular difference between the internal and external matrix layers. Considering the average anions amount between the internal and external layers of the matrix, a chloride amount equal to 1.03% and a sulfate amount equal to 2.60% were found, which is

consistent with the amounts found in real historic buildings affected by intense rising damp [43-45].

Some salt enrichment occurs also on the top part of the brick (close to the composite), but no substantial accumulation of salts was found in the brick either beneath the composite or beside. This observation confirms that the natural hydraulic lime mortar does not hinder the capillary flow. The accumulation of salts in the NHL matrix is consistent with the results found by MIP.

Interestingly, the anion amounts in the composite of NHL-SALT-BEFORE masonry joints are similar to those found in NHL-SALT samples, which means that the composite absorbs the salts from the salt laden substrate during its drying phase and hence behaves like a sort of poultice over salt contaminated masonry. This is a key aspect in the case of in situ applications, because the presence of salts in newly applied FRCMs might boost subsequent crystallization cycles in the composite due to relative humidity variations that may occur daily or seasonally.

The salt accumulation pattern in CEM specimens is completely different with respect to NHL (Fig. 14). In CEM-WAT, the amount of salts in the composite and in the brick beneath the strip is basically unaltered with respect to CEM-REF, while a slight increase is observed on each side of the FRCM strip, i.e. in the part of the brick outside the bonded area. The same pattern can be observed in CEM-SALT specimens, where the salt accumulation in the composite and in the brick beneath is limited, which confirms the low porosity alteration found in the matrix by MIP (curves almost overlap in Fig. 12a), while the highest increase of amount of salts is found in the portion of the brick outside the bonded area. A possible explanation is that the FRCM strip, due to its low porosity and thin pores (associated with a slow sorptivity), hinders the capillary flow and makes it deviate towards an easier path, i.e. through the brick. The result is that a limited amount of the saline solution flows through the composite and a low amount of salts is deposited in the matrix pores, without even forming efflorescence over the external surface (as shown in Fig. 3c and e). Conversely, the flow and the subsequent evaporation are concentrated in the brick outside the bonded area, where a higher salt accumulation is found. The fact that the presence of scarcely permeable mortars exacerbates the salt damage in the surrounding bricks is consistent with what

frequently observed on-site, as discussed in [46] and shown in the examples of Fig. 15.



Figure 15. Increase of bricks deterioration in correspondence of scarcely permeable repointing mortars, boosting the water transport through the bricks (on the left: complex of the *Corpus Domini* church, Bologna, Italy; on the right: *S. Maria delle Consolazioni* church, Este, Italy).

4. Conclusions

An accelerated laboratory test, involving wetting and drying cycles in a saline solution with sodium chloride and sodium sulfate, was used to investigate the salt crystallization resistance of FRCM composite strips applied to masonry blocks. A porous mortar (with natural hydraulic lime as binder) and a more compact mortar (with Portland cement as binder) were used as matrices for the composite strips, while the fibers (galvanized steel cords) and the masonry blocks were kept the same, in order to highlight the role of the matrix on the salt crystallization patterns and on the bond resistance of the composite. The results allowed to make the following observations:

- the type of matrix employed in the composite determines the location of the fracture surface during the single-lap shear test: at the fiber-matrix interface for NHL specimens and at the masonry-composite interface for CEM specimens. This is due to the different mechanical performance of the two mortars and is related to the hierarchy of the interfaces in the FRCM-masonry joints. Due to this, the peak load of the reference FRCM-masonry joints is very similar for both the groups of specimens, despite the different compressive strengths of the matrices;
- the different microstructure of the two mortars (higher total open porosity and mean pore

radius for NHL with respect to CEM) and their different capillary absorption velocity (more than double for NHL, compared to CEM) strongly influence the migration pattern of the saline solution during the salt crystallization cycles and the salt distribution inside the specimens. In particular, the saline solution flows through the composite strip in NHL specimens, forming efflorescence on the surface, while it flows aside the composite strip in CEM specimens, crystallizing on top of the masonry. This latter behavior is due to the much higher porosity and sorptivity of the brick with respect to CEM matrix. In both NHL and CEM specimens, the matrix of the composite is not damaged by the salt crystallization cycles, but some spots of corrosion were found in the steel cords embedded in the NHL matrix, due to the abundant chloride accumulation in the pores. For this reason, the NHL specimens exhibited a lower peak load after the cycles in the saline solution (NHL-SALT) with respect to the reference specimens (NHL-REF);

- in water saturated conditions, the bond adhesion of the composite strip to the substrate is reduced for NHL specimens, as the fracture develops at the matrix-fiber interface and hence it is affected by the ‘softening’ of the NHL matrix. In CEM specimens, as the fracture occurs in the masonry substrate, water saturation seems to lead to no consequences;
- the application of the composite strip over salt-laden masonry substrates may lead to negative consequences. In the case of NHL, the mortar quickly absorbs the salts from the substrate, becoming rich of potentially damaging salts which may lead to salt crystallization cycles in case of on-site relative humidity variations. In the case of CEM, the bond resistance is affected by the salt laden substrate, as the adhesion of the matrix to an already deteriorated substrate is reduced.

Acknowledgments

The experimental work discussed in this paper was conducted at the University of Bologna.

Technicians of the laboratory LISG (Laboratory of Structural and Geotechnical Engineering), CIRI

(Interdepartmental Centre for Industrial Research in Building and Construction), LASTM (Laboratory of Materials Science and Technology) are gratefully acknowledged for their help during the preparation of the specimens and the execution of the tests. The authors would like to express their appreciation to Kerakoll S.p.A. (Sassuolo, Italy) for providing the composite materials. Silvia Nanni is gratefully acknowledged for her support during the experimental campaign. Financial support by the Italian Ministry of Education, Universities and Research MIUR is gratefully acknowledged (PRIN2015: “Advanced mechanical modeling of new materials and structures for the solution of 2020 Horizon challenges”, prot. 2015JW9NJT 018).

References

- [1] Erder C. Our architectural heritage: from consciousness to conservation. Unesco (1986).
- [2] Babatunde SA. Review of strengthening techniques for masonry using fiber reinforced polymers. *Compos Struct*, 161 (2017), pp. 246-255.
- [3] Sassoni E, Andreotti S, Bellini A, Mazzanti B, Bignozzi MC, Mazzotti C, Franzoni E. Influence of mechanical properties, anisotropy, surface roughness and porosity of brick on FRP debonding force. *Compos Part B Eng*, 108 (2017), pp. 257-269.
- [4] Sciolti MS, Aiello MA, Frigione M. Influence of water on bond behavior between CFRP sheet and natural calcareous stones. *Compos Part B Eng*, 43 (2012), pp. 3239–3250
- [5] Maljaee H, Ghiassi B, Lourenco PB, Oliveira DV. FRP–brick masonry bond degradation under hygrothermal conditions. *Compos Struct*, 147 (2016), pp. 143–154
- [6] Trapko T. The effect of high temperature on the performance of CFRP and FRCM confined concrete elements. *Compos Part B Eng*, 54 (2013), pp. 138–145
- [7] Tedeschi C, Kwiecień A, Valluzzi MR, Zajac B, Garbin E, Binda L. Effect of thermal ageing and salt decay on bond between FRP and masonry. *Materials and Structures* 47 (12) (2014) 2051-2065.
- [8] Di Tommaso A, Focacci F, Micelli F. Strengthening historical masonry with FRP or FRCM: Trends in design approach. *Key Engineering Materials*, 747 KEM (2017), pp. 166-173.
- [9] Carozzi FG, Milani G, Poggi C, Mechanical properties and numerical modeling of fabric reinforced cementitious matrix (FRCM) systems for strengthening of masonry structures. *Compos Struct*, 107 (2014), pp. 711–725
- [10] Carabba L, Santandrea M, Carloni C, Manzi S, Bignozzi MC. Steel fiber reinforced

- geopolymer matrix (S-FRGM) composites applied to reinforced concrete structures for strengthening applications: A preliminary study. *Compos Part B Eng*, 128 (2017), pp. 83-90.
- [11] Santandrea M, Daissè G, Mazzotti C, Carloni C. An investigation of the debonding mechanism between FRCM composites and a masonry substrate. *Key Engineering Materials*, 747 KEM (2017), pp. 382-389.
- [12] Nobili A. Durability assessment of impregnated Glass Fabric Reinforced Cementitious Matrix (GFRCM) composites in the alkaline and saline environments. *Constr Build Mater*, 105 (2016), pp. 465-471.
- [13] Tedeschi C, Perego S, Valluzzi MR. Study on local effects of aggressive environmental conditions on masonry strengthened with FRCM. In: *Brick and Block Masonry: Trends, Innovations and Challenges - Proceedings of the 16th International Brick and Block Masonry Conference, IBMAC 2016*, pp. 441-450.
- [14] Aljazaeri, ZR, Myers JJ. Durability performance of FRCM composite bonded to concrete under different environmental aging conditions. In: *Proceedings of the 8th International Conference on Fibre-Reinforced Polymer (FRP) Composites in Civil Engineering, CICE 2016*, pp. 518-524.
- [15] Franzoni E, Gentilini C, Santandrea M, Zanotto S, Carloni C. Durability of steel FRCM-masonry joints: Effect of water and salt crystallization. *Mater Struct*, 50(4) (2017), Article N. 201.
- [16] Franzoni E, Gentilini C, Santandrea M, Carloni C. Effects of rising damp and salt crystallization cycles in FRCM-masonry interfacial debonding: Towards an accelerated laboratory test method. *Constr Build Mater*, 175 (2018), pp. 225-238.
- [17] Bencardino F, Carloni C, Condello A, Focacci F, Napoli A, Realfonzo R. Flexural behaviour of RC members strengthened with FRCM: State-of-the-art and predictive formulas. *Compos Part B Eng*, 148 (2017), pp. 132–148.
- [18] Sneed LH, Verre S, Carloni C, Ombres L. Flexural behavior of RC beams strengthened with steel-FRCM composite. *Eng Struct*, 127 (2016), pp. 686-699.
- [19] Napoli A, Realfonzo R. Reinforced concrete beams strengthened with SRP/SRG systems: experimental investigation. *Constr Build Mater*, 93 (2015), pp. 654-677.
- [20] Shadravan B, Tehrani FM. A review of direct shear testing configurations for bond between fiber-reinforced polymer sheets on concrete and masonry substrates. *Periodica Polytechnica Civil Engineering*, 61 (2017), pp. 740-751.
- [21] Sassoni E, Sarti V, Bellini A, Mazzotti C, Franzoni E. The role of mortar joints in FRP debonding from masonry. *Compos Part B Eng*, 135 (2018), pp. 166-174.

- [22] EN 459-1. Building lime - Part 1: Definitions, specifications and conformity criteria (2015).
- [23] Technical datasheet of GeoCalce® Fino (Kerakoll S.p.A., Italy).
- [24] EN 998-2. Specification for mortar for masonry – Part 2: Masonry mortar (2016).
- [25] Technical datasheet of GeoLite® (Kerakoll S.p.A., Italy).
- [26] EN 12190. Products and systems for the protection and repair of concrete structures - Test methods: Determination of compressive strength of repair mortar (1999).
- [27] Lubelli B, Cnudde V, Diaz-Goncalves T. et al. Towards a more effective and reliable salt crystallization test for porous building materials: Inputs from past experience. *Mater Struct* 51:55 (2018), pp. 1-21.
- [28] MS-A.1 Determination of the resistance of wallettes against sulphates and chlorides. *Mater Struct*, 31 (1998), pp. 2-19.
- [29] EN 12370. Natural stone test methods. Determination of resistance to salt crystallization (1999).
- [30] West D. Brard's test into the 21st century: Sodium sulfate soundness testing of dimension stone. In McNally, G.H. & Franklin, B.J. (eds) *Sandstone city: Sydney's dimension stone and other sandstone geomaterials*. Proceedings of a Symposium held on 7th July 2000, during the 15th Australian Geological Convention at the University of Technology. Sydney Group, Monograph, 5 (2000), pp. 138–148.
- [31] Franzoni E, Gentilini C, Graziani G, Bandini S. Towards the assessment of the shear behaviour of masonry in on-site conditions: A study on dry and salt/water conditioned brick masonry triplets. *Constr Build Mater*, 65 (2014), pp. 405-416.
- [32] Franzoni E, Gentilini C, Graziani G, Bandini S. Compressive behaviour of brick masonry triplets in wet and dry conditions. *Constr Build Mater*, 82 (2015), pp. 45–52
- [33] Verstryngne E, Adriaens R, Elsen J, Van Balen K. Multi-scale analysis on the influence of moisture on the mechanical behavior of ferruginous sandstone. *Constr Build Mater*, 54 (2014), pp. 78–90.
- [34] Vásárhelyi B, Ván P. Influence of water content on the strength of rock. *Eng Geol*, 84 (2006), pp. 70–4.
- [35] Wiederhorn SM, Freiman SW, Fuller Jr ER, Simmons CJ. Effects of water and other dielectrics on crack growth. *J Mater Sci*, 17(12) (1982), pp. 3460–78.
- [36] Zhang C, Zhao Q. Triaxial tests of effects of varied saturations on strength and modulus for sandstone. *Rock Soil Mech*, 35(4) (2014), pp. 951–8.
- [37] Wu S, Chen X, Zhou J. Influence of strain rate and water content on mechanical behavior of dam concrete. *Constr Build Mater*, 36 (2012), pp. 448–57.

- [38] EN 1015–11. Methods of test for mortar for masonry - Part 11: Determination of flexural and compressive strength of hardened mortar (1999).
- [39] EN 15801. Conservation of cultural property - Test methods - Determination of water absorption by capillarity (2009).
- [40] Sneed LH, D'Antino T, Carloni C, Pellegrino C. A comparison of the bond behavior of PBO-FRCM composites determined by single-lap and double lap shear tests. *Cement Concrete Comp*, 64 (2015), pp. 37-48.
- [41] Carloni C, D'Antino T, Sneed LH, Pellegrino C. 3-D numerical modeling of single-lap direct shear tests of FRCM-concrete joints using a cohesive contact damage approach. *J Compos Constr*, 22 (2018), pp. 1–10.
- [42] Verges-Belmin V, Siedel H. Desalination of masonries and monumental sculptures by poulticing: a review. *Restor Build Monum*, 11 (2005), pp. 1–18.
- [43] Sandrolini F, Franzoni E, Cuppini G, Caggiati L. Materials decay and environmental attack in the Pio Palace at Carpi: a holistic approach for historical architectural surfaces conservation. *Build Environ*, 42 (2007), pp. 1966–1974.
- [44] Franzoni E, Bandini S, Graziani G. Rising moisture, salts and electrokinetic effects in ancient masonries: From laboratory testing to on-site monitoring. *J Cult Herit*, 15 (2014), pp. 112-120.
- [45] Sandrolini F, Franzoni E, Vio E, Lonardoni S. Challenging transient flooding effects on dampness in brick masonry in Venice by a new technique: the narthex in St. Marco Basilica. In: Fletcher CA, Spencer T, editors. *Flooding and environmental challenges for Venice and its lagoon: state of knowledge*. Cambridge: Cambridge University Press; (2005), pp. 181–188.
- [46] Franzoni E. The role of mortars in ancient brick masonries' decay: a study in the Pio Palace at Carpi (Italy), in: *2nd Historic Mortars Conference HMC2010 and RILEM TC 203-RHM Final Workshop (RILEM Proceedings PRO 78)*, Prague, s.n, 2010, pp. 483-490.